INŽENÝRSKÁ MECHANIKA 2005

NÁRODNÍ KONFERENCE

s mezinárodní účastí

Svratka, Česká republika, 9. - 12. května 2005

ONE-DIMENSIONAL MATHEMATICAL MODEL OF THE FLOW THROUGH A COLLAPSIBLE TUBE WITH APPLICATIONS TO BLOOD FLOW THROUGH HUMAN VESSELS

Štembera V.[1], Maršík F.[2], Chlup H.[2,3]

Summary: *The simulation of the fluid flow through elastic pipes has a great application in a blood flow through human vessels – investigation of such phenomena as an atheriosclerosis generation in artery walls, the Korotkoff's sounds generation or modeling of vascular mechanical substitutes (the so called "stents") and is therefore widely studied. In this text we model the flow through collapsible pipes by the time-dependent, spatially one-dimensional model consisting of the balances of mass, momentum, and the coresponding material law. The experimental research of the problem is our aim as well – we introduce the new experimental set-up for testing the flow throw collapsible tube samples, which has been currently finished at ČVUT Praha.*

1. MODELED SYSTEM

The system we study is the Starling resistor (see Fig. 1). The main part consists of the thin-walled elastic tube of length l and the thickness h, where we assume $h << l$. The elastic tube is surrounded by two rigid channels. The upstream rigid channel has the length l_u and the downstream channel has the length l_d. The cross-sectional area of the tube is denoted by $A(x,t)$ while the cross-sectional area of the rigid parts is denoted by A_0. The fluid flows from the reservoir with the constant pressure p_S. The downstream rigid part ends with the restrictor connecting the system with zero pressure outside of the system. The flexible part of the tube is located within the box with the constant pressure p_e.

2. MATHEMATICAL FORMULATION

The model consists of three equations – the balance laws of mass, momentum, and the corresponding material relation. The equation of balance mass for an incompressible fluid with density ρ in an elastic tube of the cross-section $A = A(x,t)$ is

[1] Mathematical Institute of Charles University, Sokolovská 83, 186 75 Prague 8, Czech Republic (email: vitastembera@hotmail.com)

[2] Institute of Thermomechanics CAS, Dolejškova 5, 182 00 Prague 8, Czech Republic

[3] Czech Technical University in Prague, Faculty of Mechanical Engineering, Department of Mechanics, Zikova 4, 166 36 Prague 6, Czech Republic

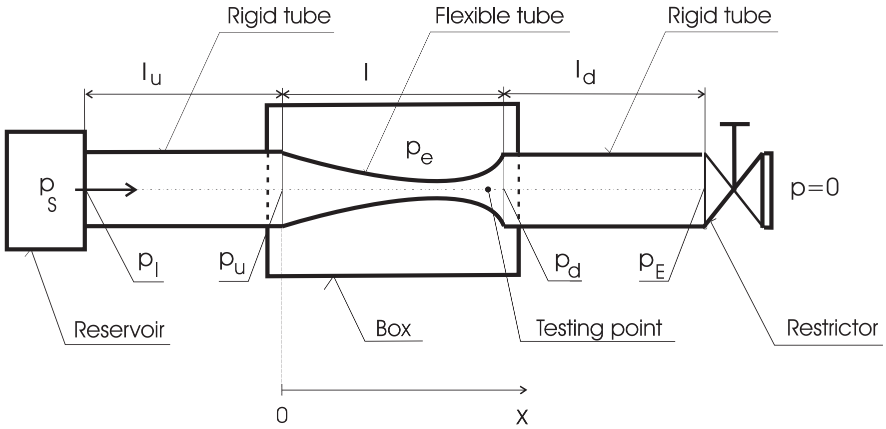

Fig. 1 The Starling Resistor

$$\frac{\partial A}{\partial t}+\frac{\partial(Av)}{\partial x}=0, \tag{2.1}$$

where $v=v(x,t)$ is the fluid velocity. The balance of momentum has the form

$$\frac{\partial v}{\partial t}+v\frac{\partial v}{\partial x}+\frac{1}{\rho}\frac{\partial p}{\partial x}=-\frac{S_0}{A_0}\frac{\lambda_f}{8}v|v|, \tag{2.2}$$

where $p=p(x,t)$ is the fluid pressure, $S_0=\pi D_0$ is the peripheral length of the internal surface. The effect of the expected flow separation is replaced by the simple viscous friction along the tube. The friction coefficient λ_f is expressed differently for the laminar flow ($\mathrm{Re}<\mathrm{Re}_{crit}$) (derived using the assumption of the Poiseuille flow) and differently for the turbulent flow ($\mathrm{Re}\geq\mathrm{Re}_{crit}$) (using an empirical formula see [2]) as follows

$$\lambda_f=\begin{cases}\dfrac{64}{\mathrm{Re}} & \text{for } \mathrm{Re}<\mathrm{Re}_{crit} \\ 1.02\left[\log(\mathrm{Re})\right]^{-2.5} & \text{for } \mathrm{Re}\geq\mathrm{Re}_{crit}\end{cases}, \tag{2.3}$$

The local Reynolds number is taken in the form

$$\mathrm{Re}=\frac{\mathrm{vA}}{\nu \mathrm{D}_0}, \tag{2.4}$$

where ν is the kinematic viscosity of the fluid. The viscoelastic properties of the elastic tube wall are taken in the form

$$\frac{T}{D_0}\frac{\partial^2 A}{\partial x^2}+p-p_e=\Phi\left(\frac{A}{A_0}\right)+\gamma\frac{\partial A}{\partial t}, \tag{2.5}$$

where γ is the tube damping and T is the tube tension and $p-p_e$ is the so-called transmural pressure. The material law (2.5) was proposed by Hayashi S. et al., 1998 ([1]).

The elastic part of the constitutive relation (2.5) is described by the function $\Phi(z)$ ([1])

$$\Phi(z)=\begin{cases} K_p\left(1-z^{-\frac{3}{2}}\right) & \text{for the collapsed state } 0<z\le 1,\\ K_E(z-1) & \text{for the inflated state } 1<z, \end{cases} \tag{2.6}$$

where K_P and K_E are stiffnesses of the flexible tube for collapsed and inflated state respectively. The second additional term in the equation (2.5) is the tensile force taking the curvature of the tube wall into account.

The material law (2.5) can be derived using the standard Hooke law. Starting with the description of an elastic body

$$\frac{\partial \tau_{ij}}{\partial x_j}=\rho\frac{\partial^2 u_i}{\partial t^2},\quad i=1,2,3\ , \tag{2.7}$$

where $\boldsymbol{\tau}$ is the stress tensor and $\mathbf{u}$ is the displacement vector, transforming equation (2.7) to cylindrical coordinates and using the assumption for the displacement $\mathbf{u}=(u_r,u_\varphi,u_z)=(u_r(z),0,0)$ we derive the material law of the form

$$\mu h\frac{\partial^2 u_r}{\partial z^2}+p-p_0=h(\lambda+2\mu)\frac{u_r}{r^2}+\rho h\frac{\partial^2 u_r}{\partial t^2}. \tag{2.8}$$

The damping term in the material law (2.5) is replaced by the inertial term on the right hand side of equation (2.8). Using the assumption of small deformations $A=\pi r^2=\pi(R_0+u_r)^2\doteq$ $\doteq A_0+S_0u_r$ denoting $x\equiv z$ we end up with

$$\frac{\mu h}{S_0}\frac{\partial^2 A}{\partial x^2}+p-p_0=\frac{h(\lambda+2\mu)}{D_0}\left(1-\frac{A_0}{A}\right)+\frac{\rho h}{S_0}\frac{\partial^2 A}{\partial t^2}. \tag{2.9}$$

The advantage of the equation (2.9) comparing to equation (2.5) is that it contains only standard elastic constants.

The flow in upstream and downstream rigid parts is modeled by following two ordinary differential equations

$$\begin{aligned} \frac{dv_u}{dt}&=\frac{p_I-p_u}{\rho l_u}-\frac{\lambda_f}{8}\frac{S_0}{A_0}v_u|v_u|,\\ \frac{dv_d}{dt}&=\frac{p_d-p_E}{\rho l_d}-\frac{\lambda_f}{8}\frac{S_0}{A_0}v_d|v_d|, \end{aligned} \tag{2.10}$$

where

$$p_S=p_I+\frac{1}{2}\rho v_u^2,\quad p_E=RA_0^2v_d|v_d|, \tag{2.11}$$

and R is the resistance of the restrictor. The pressure outside of the tube is zero.

3. NUMERICAL RESULTS

The system (2.1)-(2.6) and (2.11) was studied numerically using four different methods. All of the methods give plausibly coincident results (see Fig. 2).

The system exhibits numerically three different qualitative behaviours: the collapse of the elastic tube, the damping, and the self-excited oscillations (Fig. 2). The main question was focused on the dependence of the frequency of the self-excited oscillations on the material parameters K_P, T, see Fig 3. The three stages of behaviour: collapse, damping and self-excited oscillations are labeled by letters C, D and frequency, if the oscillations are periodic and the frequency is well determined, otherwise labeled by letter X. The region of damping at the bottom of the picture is expected due to the high stiffness of the tube.

The region of collapse at the top of the picture, i.e. when A comes to 0, is caused by the low stiffness of the tube, but it is necessary to mention that all numerical methods have difficulties converging if the cross-section A comes to value near 0. Therefore it is not clear if cross-section A as part of the real solution of the original system of equations (2.1)-(2.6) and (2.10) converges to 0 as well or if there still exist self-excited oscillations.

Surprisingly there is another damping region in the middle of the picture dividing the area of self-excited oscillations into two halves, which we denote by I (an upper one) and II (a lower one). The real tube which was meassured by Hayashi S., et al. lies in region I ($K_P = 105$ Pa, $T = 500$ Pa m, see [1]). We note that the solutions in the region I are generally more irregular comparing to the solutions in the region II. If we look at the dependence of the frequency of self-excited oscillations on parameters K_P and T we see that the frequency decreases with an increase of parameters K_P and T (an increase of the Young modulus E) in region II. In region I such dependence does not hold, which is possibly due to dominance of the nonlinear term $\Phi\left(\frac{A}{A_0}\right)$ over the term $\frac{T}{D_0}\frac{\partial^2 A}{\partial x^2}$ in this region.

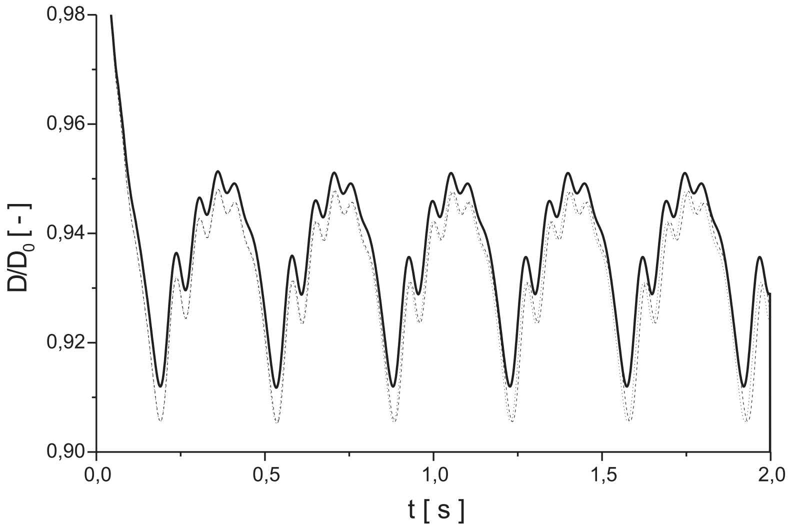

Fig. 2 Convergence of the methods for $T = 800$ Pa m, $K_P = 105$ Pa at $x = 0.955$ m (dot - the Crank-Nicholson method, dash - the Runge-Kutta method, solid - the BDF method, thick solid - the Euler method). We note that the BDF and the Euler methods coincide.

	K_p[Pa]	$\rightarrow$								
T[Pa m] $\downarrow$	30	55	80	105	130	155	180	205	230	255
300	C	C	C	C	4,58	4,63	4,66	4,67	4,68	4,68
350	C	C	X	4,21	X	X	4,68	4,71	4,71	4,72
400	X	6,86	X	X	X	X	X	X	4,79	4,78
450	X	X	X	4,65	X	4,84	X	4,87	9,65	9,58
500	X	X	X	X	X	X	4,92	9,75	9,74	D
550	X	X	X	X	5,01	4,95	9,9	D	D	D
600	X	X	X	5,09	10,03	D	D	D	D	D
650	X	X	10,13	D	D	D	D	D	D	D
700	X	X	D	D	D	D	D	3,52	3,38	3,25
750	4,04	3,96	3,76	3,59	3,43	3,23	3,07	2,94	2,83	2,7
800	3,69	3,46	3,11	2,89	2,67	2,52	2,41	2,32	2,21	D
850	2,76	2,46	2,24	2,08	1,95	1,89	D	D	D	D
900	1,86	1,67	1,45	1,35	D	D	D	D	D	D
950	X	D	D	D	D	D	D	D	D	D
1000	D	D	D	D	D	D	D	D	D	D
1050	D	D	D	D	D	D	D	D	D	D
1100	D	D	D	D	D	D	D	D	D	D

Fig. 3 Qualitative behaviour of the model for different values of parameters T and K_p for ν=1.004 × 10^{-6} $m^2 s^{-1}$ (*C* - collapse of the tube, *D* - damping of the tube, *value* - the frequency of the self-excited oscillations [Hz], *X* - aperiodic self-excited oscillations).

The system of equations (2.1)-(2.4), (2.6) and (2.10) with material law (2.9) instead of material law (2.5) was studied numerically as well. Only the damping state of behaviour were observed – the system fails to exhibit the self-excited oscillations.

4. EXPERIMENTAL SET-UP

The experimental research of the problem is also our aim. The new experimental set-up for testing the flow throw collapsible tube samples has been currently finished at ČVUT Praha. The diagram of the experimental setup is on Fig 4. The set-up is equiped by two elements homogenizing the flow located at the begining and at the end of the collapsible tube sample. The detail of the box surrounding the collapsible tube sample is depicted on Fig. 5.

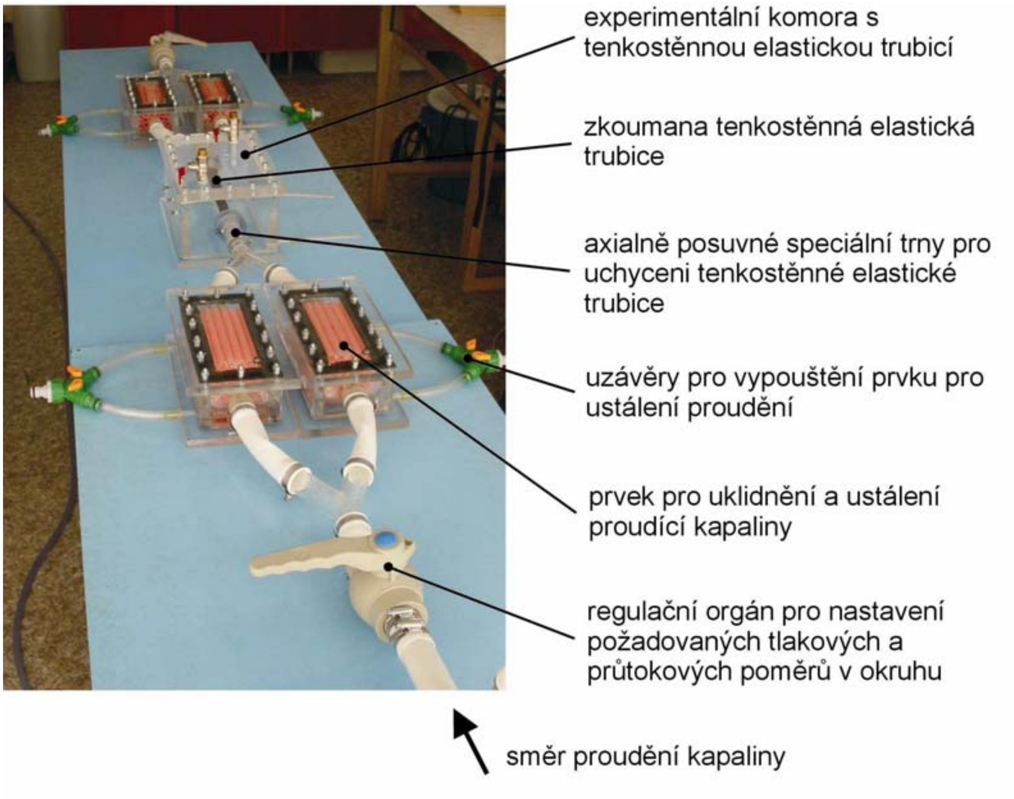

Fig. 4 The diagram of the experimental set-up. The box surrounding the collapsible tube is surrounded by two elements homogenizing the flow.

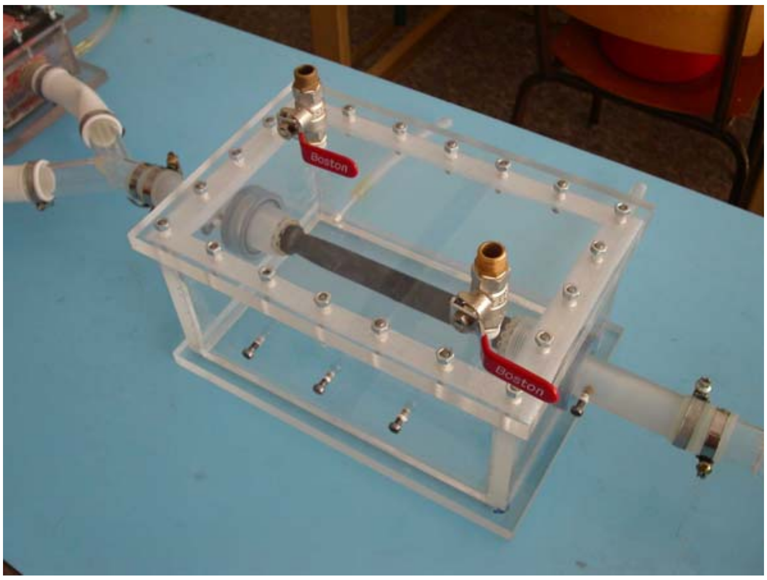

Fig. 5 The box surrounding the collapsible tube sample in detail.

5. ACKNOWLEDGEMENTS

This research was supported by the following project: PP05-281, Interakce kapaliny s pevnou a pohyblivou stěnou v oblasti biomechaniky, Institute of Thermomechanics CAS.

6. REFERENCES

[1] Hayashi S., Hayase T., Kawamura H.: *Numerical Analysis for Stability and Self-Exited Oscillation in Collapsible Tube Flow*, J. of Biomech. Eng. **Vol. 120**, (1998) 468-475.

[2] Colebrook C.F.: *Turbulent Flow in Pipes with Particular Reference to the Transition Region Between the Smooth and Rough Pipe Law*, J. Institute Civil Eng., (1939).